Carbohydrate Polymers 77 (2009) 457–463

Contents lists available at ScienceDirect

Carbohydrate Polymers

journal homepage: www.elsevier.com/locate/carbpol

# Synthesis of bacterial celluloses in multiwalled carbon nanotube-dispersed medium

Won-Il Park [a], Hun-Sik Kim [a], Soon-Min Kwon [a], Young-Ho Hong [b], Hyoung-Joon Jin [a,*]

[a] Department of Polymer Science and Engineering, Inha University, Incheon 402-751, Republic of Korea
[b] Food Ingredient Center, CJ Foods R&D, CJ CheilJedang Corp., Seoul 152-050, Republic of Korea

ARTICLE INFO

*Article history:*
Received 17 May 2008
Accepted 16 January 2009
Available online 31 January 2009

*Keywords:*
Bacterial cellulose
*Gluconacetobacter xylinum*
Multiwalled carbon nanotubes
Green fluorescent protein
Toxicity

ABSTRACT

Carbon nanotubes are considered to be the ideal multi-functional filler, although there is some debate regarding their toxicity for bio-related applications. The bacteria, *Gluconacetobacter xylinum*, which produce bacterial cellulose, were cultured in a multiwalled carbon nanotube (MWCNT) dispersed Hestrin and Schramm (HS) medium by shaking incubation. The MWCNTs were functionalized with polyethylene glycol to prepare a stable MWCNT-dispersed HS medium and its stability was characterized by measuring the transmittance of a pulsed near infrared light. To investigate the toxicity of the MWCNTs to bacteria, we also introduced a green fluorescent protein gene into the bacteria and observed the fluorescence via confocal microscopy to confirm the presence of live bacteria in the MWCNT-dispersed HS medium. On the bases of the electron microscopy observations, a substantial number of MWCNTs were found to be well-dispersed and attached to the surface of the bacterial cellulose fibrils.



## 1. Introduction

One of the major areas of carbon nanotubes (CNTs) research is the field of biomedical materials and devices. Many applications for CNTs have been proposed, including biosensors (Male, Hrapovic, Santini, & Luong, 2007), scaffolds (Correa-Duarte et al., 2004), drug delivery vehicles (Prato, Kostarelos, & Bianco, 2007), and novel biomaterials (Kam & Dai, 2005; Lu, Maragakis, & Kaxiras, 2005; Lu et al., 2004). However, before such materials can be incorporated into new and existing biomedical devices, the toxicity and biocompatibility of CNTs need to be thoroughly investigated (Abarrateggi et al., 2008; Coleman, Khan, Blau, & Gun'ko, 2006; Smart, Cassady, Lu, & Martin, 2006). Kang et al. reported that the damage to Escherichia coli cell membranes resulting from their direct contact with single-walled carbon nanotube aggregates is the likely mechanism leading to bacterial cell death (Kang, Pinault, Pfefferle, & Elimelech, 2007). Magrez et al. have shown that multiwalled carbon nanotubes (MWCNTs) have toxicity to lung tumor cells in a nanotube size-dependent manner (Magrez et al., 2006). The toxicity of CNTs to human cells has been observed to vary with the functionalization of the CNTs and the concentration of the solubilizing agent (i.e., surfactants), as well as with the physicochemical properties of the CNTs such as their structure, diameter, purity (e.g., %metal), and defect level (Chen et al., 2006; Karakoti, Hench, & Seal, 2006; Sayes et al., 2006). As a solution to the cellular toxicity of CNTs, Qiao et al. used a polyaniline/CNT composite as the anode material of microbial fuel cells (Qiao, Li, Bao, & Bao, 2007).

Owing to its high porosity, high crystallinity, water absorbance, mechanical properties, formability, and biocompatibility, bacterial cellulose has also recently attracted a great deal of attention for bio-related applications (Czaja, Krystynowicz, Bielecki, & Brown, 2006; Czaja, Young, Kawecki, & Brown, 2007; Jung et al., 2008; Klemm, Schumann, Udhardt, & Marsch, 2001; Yoon, Jin, Kook, & Pyun, 2006). For instance, bacterial cellulose has been successfully used for wound dressings and for vascular implants. The potential of bacterial cellulose for in vitro and in vivo tissue regeneration also continues to be explored and shows great promise. *Gluconacetobacter xylinum* (*G. xylinum*) is a bacterial cellulose producer and its insoluble bacterial cellulose aggregates to form different shapes. In addition, its bacterial cellulose yield, structure, and properties vary depending on the cultivation methods, such as stationary culture and agitated culture in different kinds of reactors. Furthermore, the synthesized cellulose is directly influenced by the numerous types of reagents that can be added to the medium. For example, in order to increase the bacterial cellulose productivity, agar (Bae, Sugano, & Shoda, 2004) or sodium alginate (Zhou, Sun, Hu, Li, & Yang, 2007) can be mixed with the culture medium. Recently, the effect on the structure of cellulose microfibrils was also investigated in the static culture medium containing the acid-treated MWCNTs (Yan et al., 2008).

In this study, to investigate the toxicity of the MWCNTs to the bacteria during culturing, we introduced a green fluorescent protein (GFP) gene into the bacterial cellulose cells and observed the fluorescence using confocal microscopy to confirm the presence of live cells. The bacterium was cultured on an MWCNT-dispersed Hestrin and Schramm (HS) medium by shaking incubation. To prepare a stable MWCNT-dispersed HS medium, the MWCNTs

* Corresponding author. Tel.: +82 32 860 7483; fax: +82 32 865 5178.
*E-mail address:* hjjin@inha.ac.kr (H.-J. Jin).

0144-8617/$ - see front matter © 2009 Elsevier Ltd. All rights reserved.
doi:10.1016/j.carbpol.2009.01.021

were functionalized with polyethylene glycol (PEG). Furthermore, the morphology of the bacteria cellulose cultured in the MWCNT-dispersed HS medium was observed via scanning electron microscopy and transmission electron microscopy.

## 2. Experimental

### 2.1. Materials

The MWCNTs (Iljin Nanotech Co., Korea) used in this study were synthesized by a thermal chemical vapor deposition (CVD) method. The purity of the pristine MWCNTs, as received, was >95%. Thionyl chloride ($SOCl_2$, Fluka) was used as received. Polyethylene glycol (PEG, $M_w$ = 600 g/mol, Aldrich) was used without further purification.

### 2.2. Preparation of PEG-functionalized MWCNTs

To eliminate impurities from the MWCNTs (such as metallic catalysts), the nanotubes were treated in a mixture of 3 M $HNO_3$ and 1 M $H_2SO_4$ at 60 °C for 24 h, followed by refluxing in 5 M HCl at 120 °C for 6 h. The purity of the acid-treated MWCNTs was measured to be 99% using thermogravimetric analysis (TGA, Q50, TA instruments, UK). These acid treatments are known to introduce carboxylic and hydroxyl functional groups onto the surfaces of the MWCNTs (MWCNTs-COOH) (Kim, Park, Yoon, & Jin, 2007). The MWCNTs-COOH were filtered and washed with a large amount of distilled water and then vacuum dried at room temperature overnight. The MWCNTs-COOH were reacted with excess $SOCl_2$ for 24 h under reflux, and the residual $SOCl_2$ was subsequently removed by reduced pressure distillation in conjunction with a liquid nitrogen trap, yielding acyl-chloride-functionalized MWCNTs (MWCNTs-COCl). The MWCNTs-COCl were mixed with 100 ml of PEG and stirred at 100 °C for 24 h and 1 atm. The resulting reaction medium was dissolved in excess distilled water and vacuum-filtered three times through a 0.45 μm PTFE membrane to yield the PEG-functionalized MWCNTs (MWCNTs-PEG) (Kong, Gao, & Yan, 2004).

### 2.3. Preparation of bacterial cellulose pellets

*Gluconacetobacter xylinum* BRC5 was obtained from Yonsei University and used to produce the bacterial cellulose pellets. The bacterium was cultured on HS medium by shaking incubation. The medium was composed of 2% (w/v) glucose, 0.5% (w/v) yeast extract, 0.5% (w/v) bacto-peptone, 0.27% (w/v) disodium phosphate, and 0.115% (w/v) citric acid. Cells pre-cultured in a test tube containing a small cellulose pellicle on the surface of the medium were inoculated into a 50 ml Erlenmeyer flask containing 20 ml of the HS medium. The MWCNTs-PEG was mixed in 100 ml of HS medium. The MWCNTs-PEG solution was sonicated in a bath (Kodo Technical Research Co., Korea) with a nominal frequency of 28 kHz and a power of 600 W for 1 h at 25 °C. The MWCNTs-PEG dispersion has a black ink color, and the MWCNTs were well-dispersed and stable in the HS medium. The cells pre-cultured in the 50 ml Erlenmeyer flask were inoculated into a 500 ml Erlenmeyer flask containing 200 ml of the MWCNTs dispersed in HS medium. The flasks were incubated under shaking (100 rpm) at 30 °C for 7 days.

### 2.4. Plasmid and DNA manipulation

*Escherichia coli* strains DH5α and *G. xylinum* BRC5 were used as host cells for construction. The vector plasmid pMV24 was obtained from Mitsukan Group Co., Ltd (Aichi, Japan) (Fukaya et al., 1989; Kondo, Beppu, & Horinouchi, 1995). T4 DNA ligase, DNA polymerase, dNTP, chemicals for PCR, and restriction enzyme were purchased from Takara Biomedicals (Shiga, Japan); the genomic tip and plasmid miniprep kit were from Qiagen (Hilden, Germany); the electrophoresis reagents were from Bio-Rad (Richmond, CA); and the oligonucleotides were synthesized by Cosmo Co. (Seoul, Korea). We generated a construct for the expression of the green

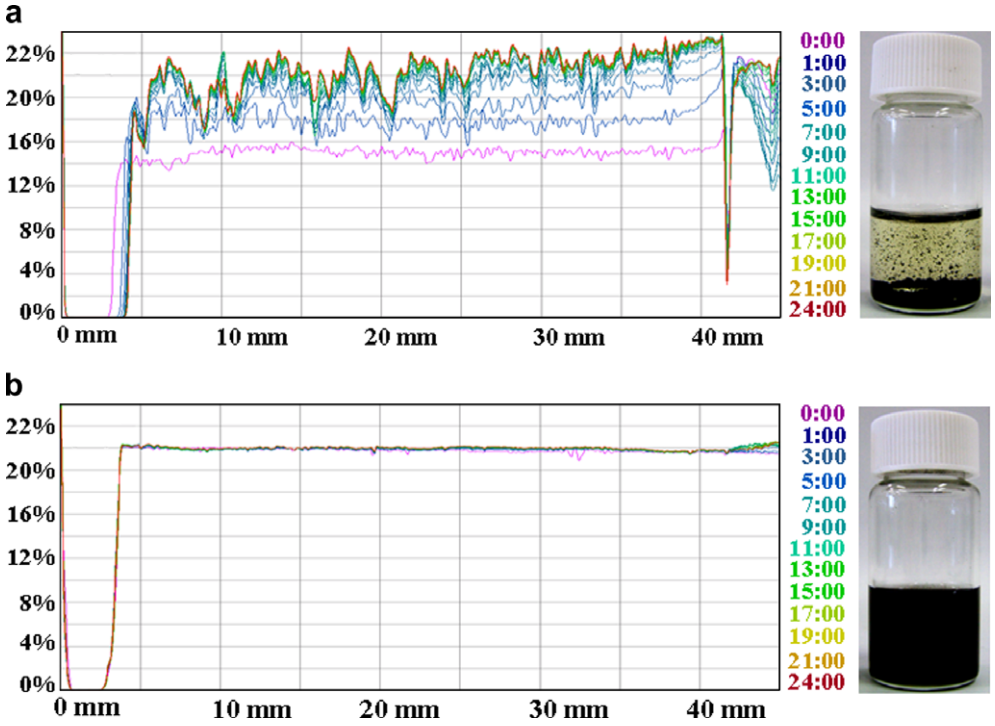


**Fig. 1.** Transmittance of (a) pristine MWCNTs and (b) MWCNTs-PEG in HS medium.

fluorescence protein (GFP) and the Kanamycin resistance ($Km^r$) gene in *G. xylinum*. First, we obtained the GFP genes and $Km^r$ genes by using PCR (denaturation at 94 °C for 30 s, annealing at 57 °C for 30 s, extension at 72 °C for 1 min, and a final extension step of 5 min at 72 °C) with the specific primer (EGFP F, EcoRI: CGGAATTC CAAGGAGATGGTGAGCAAGGGCG-AGGAG, EGFP R, pstI: AAGGCTG CAGTTACTTGTACAGCTCGTCCATGC). Each PCR product was purified on a 1% (w/v) agarose gel using a QIAEX II gel extraction kit (Qiagen). After the purification of the PCR products, the EGFP gene was subcloned into two restriction enzyme sites (EcoRI and pstI) of the pMV24 *E. coli–Gluconacetobacter* shuttle vector, and the $Km^r$ genes were subsequently inserted into the pstI site of the EGFP-containing pMV24 vector. *Gluconacetobacter* strains were transformed by the electroporation method. The pulse was delivered by a Gene-Pulser (Bio-Rad Laboratories, Richmond, California) set at 25 μF and normally at 2.0 kV. The cuvette was connected in -parallel to a 200-Ω resistor (pulse controller; Bio-Rad), resulting in time constants of 4.5–5.0 ms. The nucleotide sequence was determined by Macrogen Co. (Seoul, Korea). After culturing with the optimal growth conditions for *G. xylinum*, we confirmed the EGFP gene expression via confocal laser scanning microscopy (MRC-1024, Bio-Rad, UK).

### 2.5. Characterization

The infrared spectra of the MWCNTs and PEG-functionalized MWCNTs were measured using Fourier transformed infrared spectroscopy (FT-IR, VERTEX 80v, Bruker Optics, Germany). Each spectrum for the samples was acquired in transmission mode by the accumulation of 64 scans with a resolution of 4 $cm^{-1}$ and a spectral range of 4000–400 $cm^{-1}$. We also measured the stability of the pristine MWCNTs and MWCNTs-PEG in an HS medium using a Turbiscan (Turbiscan Lab, France) at 25 °C for 24 h. The MWCNT-dispersions were poured into 30 ml cylindrical glass vials to a height of approximate 55 mm. The stability of the MWCNT-dispersions was monitored by measuring the transmittance and back scattering of a pulsed near infrared light ($\lambda$ = 880 nm) (Terayama, Hirota, Yoshimura, & Esumi, 2002). The transmittance detector received the light which passed through the dispersion at an angle of 180° with respect to the source, while the back scattering detector received the light scattered backwards by the dispersion at an angle of 45°. The detection head scanned the entire height of the sample, acquiring the transmittance and back scattering data in steps of 40 mm every 1 h for 24 h. In this study, the back scattering data was not considered, because the MWCNT-dispersed HS medium had a jet black color and absorbed almost all of the back scattered light (Kim, Park, Kang, & Jin, 2008). Wide-angle X-ray diffraction (WAXD, DMAX-2500, Rigaku, Japan) was used to characterize the bacterial cellulose structure. Cu-$K_\alpha$ radiation was utilized ($\lambda$ = 0.154 nm) and the 2$\theta$ angle was set between 5° and 40°. The crystallinity index was calculated as $Cr = (I_{002} - I_{am})/I_{002}$, where $I_{002}$ is the overall intensity of the peak at a 2$\theta$ value of about 22° and $I_{am}$ is the intensity of the baseline at a 2$\theta$ value of about 18° (Moon, Park, Chun, & Kim, 2006). The crystallite size was calculated by the Scherrer equation (Mihranyan, Llagostera, Karmhag, Stromme, & Ek, 2004). The morphology of the bacterial cellulose was imaged using a field emission scanning electron microscope (FESEM, S-4300, Hitachi, Japan) and transmission electron microscope (TEM, CM200, Philips, Japan). The bactericidal activity in the MWCNT-dispersed HS medium was observed through observa-

**Table 1**
The *d*-spacings, crystalline sizes and crystallinity of the bacterial cellulose prepared by shaking culture systems.

| Bacterial cellulose | *d*-Spacings (nm) | | | Crystalline sizes (nm) | Crystallinity (%) |
|---|---|---|---|---|---|
| | $d_1$ | $d_2$ | $d_3$ | $cr_3$ | $c$ |
| HS medium | 0.62 | 0.58 | 0.40 | 6.39 | 75.9 |
| MWCNT-dispersed HS medium | 0.63 | 0.54 | 0.40 | 5.97 | 34.2 |

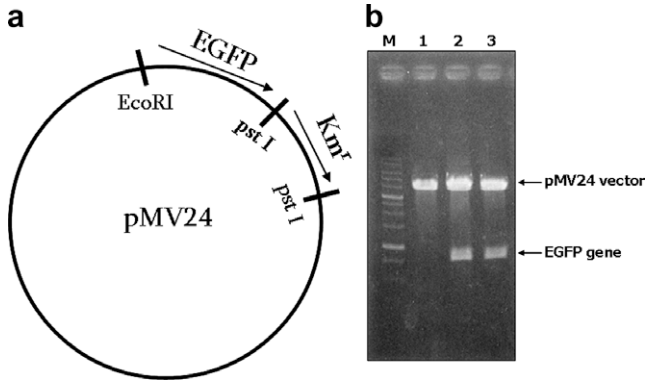


**Fig. 3.** (a) Construction scheme and (b) plasmid pattern of EGFP-pMV24 shuttle vector for the overexpression of GPF protein in *G. xylinum* (M, 1 kb leader; 1, pMV24 vector; 2 and 3, EGFP-pMV24 vector).

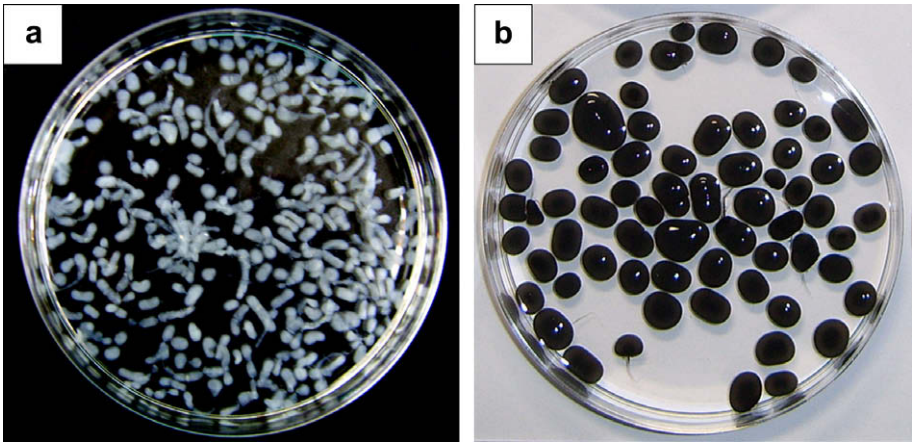


**Fig. 2.** Photographs of bacterial cellulose pellets synthesized in (a) HS medium and (b) MWCNT-dispersed HS medium in a shaking culture system at 30 °C for 7 days (100 rpm).

tions using a fluorescence microscope (Axioskop2MAT, Carl Zeiss, Thornwood, NY). The excitation wavelength was 445–495 nm and the observation filter had a long-pass filter transparent for wavelengths above 515 nm.

## 3. Results and discussion

First, to prepare stable MWCNTs in an HS medium, the MWCNTs were functionalized with PEG. The acid-treated MWCNTs (MWCNTs-COOH) were reacted first with excess $SOCl_2$ and then with excess PEG. Evidence for their functionalization is provided by the FT-IR spectra. The peaks due to the carbonyl stretches of these materials show good correspondence to the expected structure of the MWCNTs (Zhao, Hu, Yu, Perea, & Haddon, 2005). The spectrum of the MWCNTs-COOH shows a signal at 1705 $cm^{-1}$, which is attributed to the carbonyl stretching of the carboxylic acid group (Zhao et al., 2005). The spectrum of the MWCNTs-PEG shows a signal at 1740 $cm^{-1}$, which can be assigned to the carbonyl vibration of the ester bonding (Zhao et al., 2005). The functionalized PEG content in the MWCNTs-PEG was approximately 15.2 wt% which was determined by TGA.

We obtained a well-dispersed HS medium containing MWCNTs via their functionalization with PEG. The concentration of the MWCNTs concentration was 0.03 wt% for forming a homogeneous dispersion of MWCNTs in HS medium. The resulting dispersions were homogeneous and stable, and jet black colored. Moreover, the MWCNTs-PEG in the dispersions did not sediment to the bottom, even when they were left standing for a month, whereas the pristine MWCNTs dispersed in the HS medium completely sedimented in a couple of hours. Fig. 1 shows the transmittance profiles obtained from the dispersions of MWCNTs over a period of 24 h. In the transmittance profiles, the curves of the MWCNTs-PEG dispersion in the HS medium are constant over time, whereas those of the pristine MWCNTs dispersion rapidly increased. These results indicate that the MWCNTs-PEG were more stable than was the pristine MWCNT-dispersion.

Most of the *G. xylinum* strains used worldwide in research synthesize cellulose statically in the form of a gelatinous membrane. When these cultures are grown in agitated conditions, a poor yield is often obtained. Considering the properties of our *G. xylinum* strain, especially its outstanding genetic stability, it is possibly one of the best available strains to apply using large-scale agitated and shaking culture systems. In the case of pure bacterial cellulose, white pellets are synthesized by a shaking culturing method (Fig. 2). The *G. xylinum* strain in the shaking culture produces cellulose in the form of characteristic pellets after 7 days of culture, as shown in Fig. 2. Black colored bacterial cellulose pellets are observed in the MWCNT-dispersed HS medium. The black colored bacterial cellulose pellets are larger than the pure bacterial cellulose pellets.

In order to compare the changes of the microstructure in the bacterial cellulose under the two different culture conditions, and in particular to estimate if the MWCNTs cause any disturbance to the crystallization process, X-ray diffraction was used. The X-ray diffraction patterns taken for both bacterial cellulose samples, which represent a typical profile of cellulose I (Tokoh, Takabe,

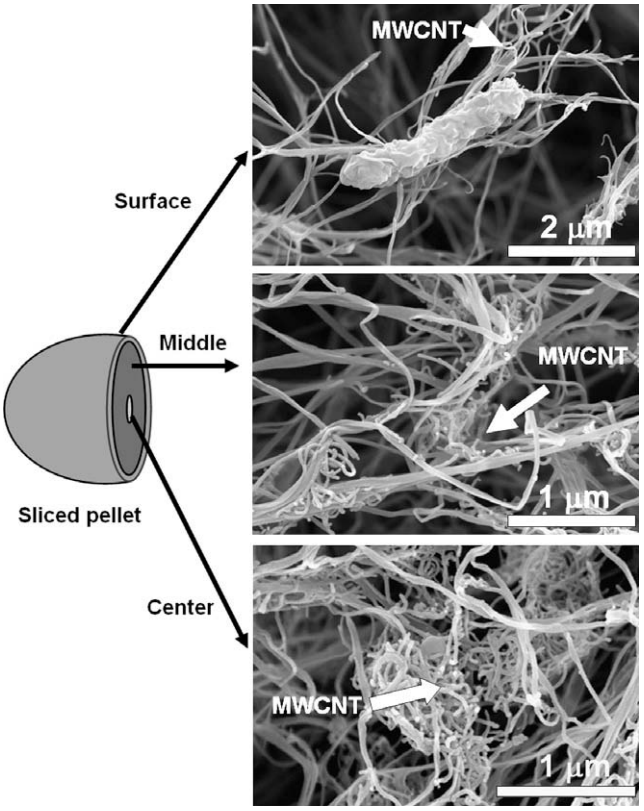


**Fig. 5.** FESEM images of bacterial cellulose synthesized in MWCNT-dispersed HS medium: surface layer, middle layer and center layer under a shaking culture system at 30 °C for 7 days (100 rpm).

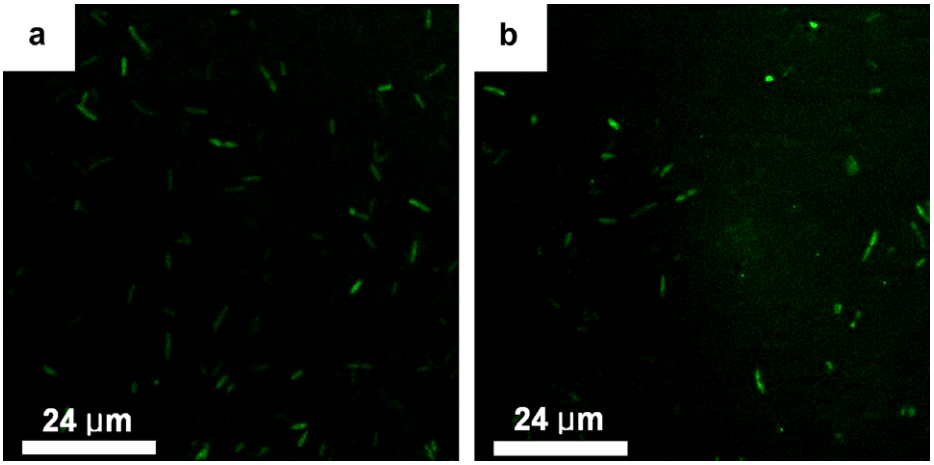


**Fig. 4.** Fluorescent images of bacteria: EGFP gene expressed cells (a) in HS medium and (b) in MWCNT-dispersed HS medium under a shaking culture system at 30 °C for 7 days (100 rpm).

Fujita, & Saiki, 1998). A quantitative analysis of the reflections corresponding to all three peaks in the X-ray profiles revealed that they have the same *d*-spacing (Table 1). Comparison of the $2\theta$ angle values also revealed that the $(1\bar{1}0)$ and $(110)$ reflections are positioned closer together in the case of the bacteria cultivated in HS medium than in the cellulose profile from the cellulose grown in the MWCNT-dispersed HS medium. As a result, it appears that the MWCNTs do not cause any significant change in the bacterial cellulose structure. In addition, the crystallinity index calculated based on the X-ray profiles revealed a reduction in crystallinity for the MWCNT-dispersed HS medium cultured cellulose samples. Yan et al. reported that the change to crystallinity resulting from their interaction between sub-elementary bacterial cellulose and MWCNT (Yan et al., 2008). The crystallite sizes calculated for the three peaks using the Scherrer formula are shown in Table 1. The results clearly show that the bacterial cellulose from the MWCNT-dispersed HS medium has smaller crystallite sizes. The crystallinity indexes of the bacterial cellulose in the HS medium and in the MWCNT-dispersed HS medium are 75.9% and 34.2%, respectively. The conditions of MWCNTs absorption during growth appear to strongly interfere with the process of nascent nanofibril crystallization.

To investigate the toxicity of the nanotubes to live cells, we introduced an EGFP gene into the bacterial cellulose cells and observed their fluorescence using confocal microscopy. To introduce the EGFP gene into the *G. xylinum* cells, we constructed a pMV24 shuttle vector harboring EGFP genes. First, we tested various antibiotics for the gene selection marker. Since *G. xylinum* grew slightly under ampicillin (50 μg/ml), we inserted $Km^r$ genes into the pMV24 shuttle vector (Fig. 3a). After gaining the gene by PCR, EGFP genes and $Km^r$ genes were inserted into the pMV24 vector and then transformed into *E. coli* DH5α. Colonies resistant to ampicillin (50 μg/ml) and Kanamycin (25 μg/ml) were selected as transformants. We selected the EGFP-pMV24 plasmid. After plasmid harvesting, plasmids were introduced into the *G. xylinum* cells by electroporation. We successfully constructed an EGFP-pMV24 vector system (Fig. 3b). However, the expression level of the EGFP genes was not high. Therefore, it was necessary to observe the expression of the EGFP gene by using confocal microscopy. Thus, with the EGFP-pMV24 vector, it was possible to investigate the production of cellulose on the basis of the fluorescence.

Due to their very weak self-fluorescence, CNTs themselves are not easily identified by a fluorescence detector (Gogoi et al., 2006). Fluorescence microscopic observations showed that the cells transfected with EGFP were labeled with green fluorescence in the cells. Fig. 4 shows the fluorescence microscopic images of the bacterial cellulose cells in the HS medium and MWCNT-dispersed HS medium. As is clear from the pictures (Fig. 4), there were similar populations of bacteria on the pellet surfaces. These results show that the grafted PEG molecules decreased the toxicity and improved the stability of the MWCNTs (Chattopadhyay, de Jesus Cortez, Chakraborty, Slater, & Billups, 2006; Zhao et al., 2005). The FESEM images of the freeze-dried pellet showed that the water-swollen cellulose gel contained a random assembly of nanofibrils with a diameter of approximately $43 \pm 11$ nm ($n = 50$)

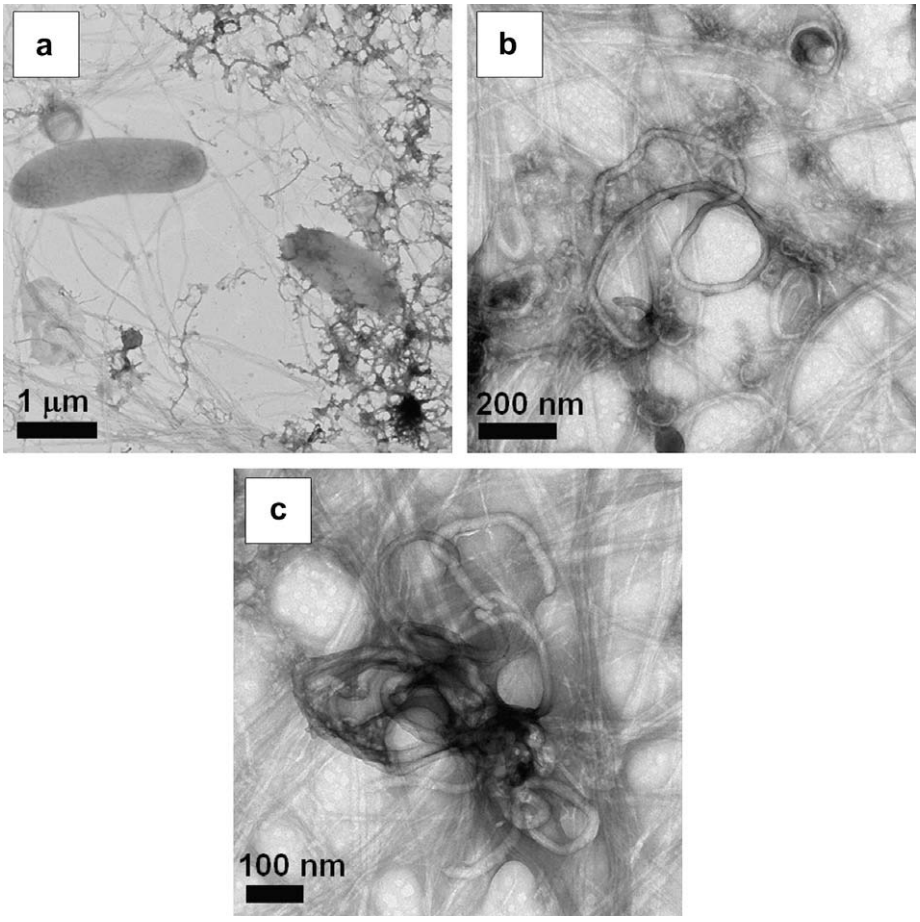


**Fig. 6.** TEM images of bacteria cellulose synthesized in MWCNT-dispersed HS medium: (a) surface layer, (b) middle layer and (c) center layer under a shaking culture system at 30 °C for 7 days (100 rpm).

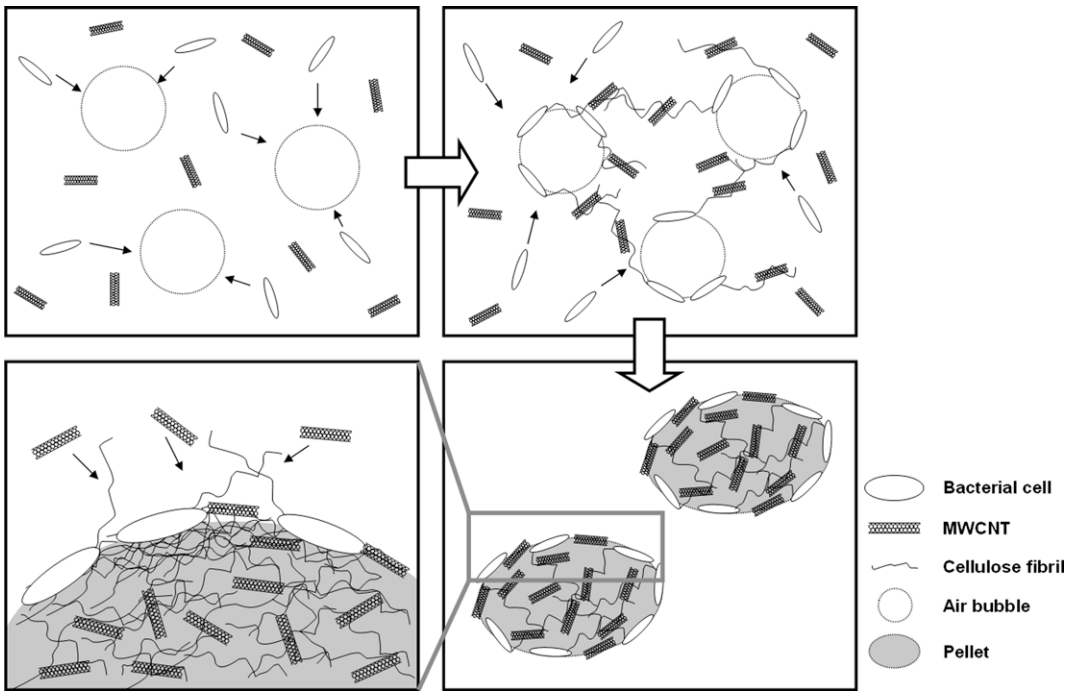


**Fig. 7.** Schematic representation of bacterial cell growth in the presence of MWCNTs under a shaking culture system.

(Fig. 5). We classified the bacterial cellulose pellets into three classes according to their location (surface layer, middle layer, and center layer). At the surface layer, the bacteria cells are located beside the nanofibrils, as shown in Fig. 5. The middle and center layer regions show a more compact structure than that of the surface layer. In addition, a substantial number of MWCNTs are well-dispersed and attached to the bacterial cellulose.

We also observed the morphology of the three layer bacterial cellulose by TEM, as shown in Fig. 6. In the surface layer (Fig. 6a), the bacteria cells, bacterial cellulose, and MWCNTs were observed. However, only bacterial cellulose and MWCNTs were observed in the middle and center layers (Fig. 6b and c). These results can be attributed to the introduction of air for the purpose of sustaining the bacteria cells on the surface part of the bacterial cellulose pellet. A similar phenomenon was also reported by Czaja, Romanovicz, and Brown (2004). According to these results, it appears that particular arrangements of bacteria cells are introduced into the fresh medium. The bacteria cells then become attached near the surfaces of air bubbles existing in the agitated liquid, and they start to reproduce and synthesize cellulose ribbons, eventually forming a more compact structure. These hypotheses regarding the surface distribution of the bacteria cells accords well with our results. A possible schematic representation of the bacteria cell growth in the MWCNT-dispersed HS medium is shown in Fig. 7. First, the bacteria cells attach to air bubbles in the MWCNT-dispersed HS medium. The attached bacteria cells reproduce and synthesize cellulose fibrils, and then disperse the MWCNTs absorbed on the fibrils. The MWCNT absorbed cellulose fibrils subsequently aggregate, forming small clusters. The synthesis of cellulose and absorption of MWCNTs continuously progress until a more compact structure is formed.

## 4. Conclusions

In this study, the bacterial cellulose was cultured in an MWCNT-dispersed HS medium to investigate the effect of MWCNTs, especially their toxicity to bacteria (*G. xylium*). The GFP gene was introduced into bacterial cellulose cells and their fluorescence was observed via confocal microscopy to judge their activity. The confocal microscopic images of the bacterial cellulose cells cultured in the HS medium and MWCNT-dispersed HS medium showed no difference in terms of the bacteria populations on the pellet surfaces. In addition, we successfully prepared the culture medium containing stably dispersed MWCNTs by the introduction of PEG on their surfaces, which was confirmed by means of Turbiscan. A substantial number of MWCNTs were well-dispersed and attached to the cellulose by observing the morphology of the cellulose pellets synthesized in an MWCNT-dispersed HS medium.

## Acknowledgements

We thank Prof. Yu Ryang Pyun (Yonsei University, Korea) for the EGFP gene cloning and Mitsukan Group Co., Ltd (Aichi, Japan) for supplying the vector plasmid, pMV24. This work was supported by a grant (Code # 200810FTH010102001) from BioGreen21 Program, Rural Development Administration, Republic of Korea.

## References

Abarrateggi, A., Gutiérrez, M., Moreno-Vicente, M., Hortigüela, M., Ramos, V., López-Lacomba, J., et al. (2008). Multiwall carbon nanotube scaffolds for tissue engineering purposes. *Biomaterials, 29*, 94–102.

Bae, S., Sugano, Y., & Shoda, M. (2004). Improvement of bacterial cellulose production by addition of agar in a jar fermentor. *Journal of Bioscience and Bioengineering, 97*, 33–38.

Chattopadhyay, J., de Jesus Cortez, F., Chakraborty, S., Slater, N. K. H., & Billups, W. E. (2006). Synthesis of water-soluble PEGylated single-walled carbon nanotubes. *Chemistry of Materials, 18*, 5864–5868.

Chen, X., Tam, U. C., Czlapinski, J. L., Lee, G. S., Rabuka, D., Zettl, A., et al. (2006). Interfacing carbon nanotubes with living cells. *Journal of the American Chemical Society, 128*, 6292–6293.

Coleman, J. N., Khan, U., Blau, W. J., & Gun'ko, Y. K. (2006). Small but strong: A review of the mechanical properties of carbon nanotube–polymer composites. *Carbon, 44*, 1624–1652.

Correa-Duarte, M. A., Wagner, N., Rojas-Chapana, J., Morsczeck, C., Thie, M., & Giersig, M. (2004). Fabrication and biocompatibility of carbon nanotube-based 3D networks as scaffolds for cell seeding and growth. *Nanoletters, 4*, 2233–2236.

Czaja, W., Krystynowicz, A., Bielecki, S., & Brown, R. M. Jr., (2006). Microbial cellulose – the natural power to heal wounds. *Biomaterials, 27*, 145–151.

Czaja, W., Romanovicz, D., & Brown, R. M. Jr., (2004). Structural investigations of microbial cellulose produced in stationary and agitated culture. *Cellulose, 11*, 403–411.

Czaja, W. K., Young, D. J., Kawecki, M., & Brown, R. M. Jr., (2007). The future prospects of microbial cellulose in biomedical applications. *Biomacromolecules, 8*, 1–12.

Fukaya, M., Tayama, K., Tamaki, T., Tagami, H., Okumura, H., Kawamura, Y., et al. (1989). Cloning of the membrane-bound aldehyde dehydrogenase gene of *Acetobacter polyoxogenes* and improvement of acetic acid production by use of the cloned gene. *Applied and Environmental Microbiology, 55*, 171–176.

Gogoi, S. K., Gopinath, P., Paul, A., Ramesh, A., Ghosh, S. S., & Chattopadhyay, A. (2006). Green fluorescent protein-expressing *Escherichia coli* as a model system for investigating the antimicrobial activities of silver nanoparticles. *Langmuir, 22*, 9322–9328.

Jung, R., Kim, H.-S., Kim, Y., Kwon, S.-M., Lee, H. S., & Jin, H.-J. (2008). Electrically conductive transparent papers using multiwalled carbon nanotubes. *Journal of Polymer Science. Part B: Polymer Physics, 46*, 1235–1242.

Kam, N. W. S., & Dai, H. (2005). Carbon nanotubes as intracellular protein transporters: Generality and biological functionality. *Journal of the American Chemical Society, 127*, 6021–6026.

Kang, S., Pinault, M., Pfefferle, L. D., & Elimelech, M. (2007). Single-walled carbon nanotubes exhibit strong antimicrobial activity. *Langmuir, 23*, 8670–8673.

Karakoti, A. S., Hench, L. L., & Seal, S. (2006). The potential toxicity of nanomaterials – the role of surfaces. *Journal of the Minerals, Metals and Materials Society, 58*, 77–82.

Kim, H.-S., Park, W. I., Kang, M., & Jin, H.-J. (2008). Multiple light scattering measurement and stability analysis of aqueous carbon nanotube dispersions. *Journal of Physics and Chemistry of Solids, 69*, 1209–1212.

Kim, H.-S., Park, B. H., Yoon, J. S., & Jin, H.-J. (2007). Thermal and electrical properties of poly(L-lactide)-graft-multiwalled carbon nanotube composites. *European Polymer Journal, 43*, 1729–1735.

Klemm, D., Schumann, D., Udhardt, U., & Marsch, S. (2001). Bacterial synthesized cellulose – artificial blood vessels for microsurgery. *Progress in Polymer Science, 26*, 1561–1603.

Kondo, K., Beppu, T., & Horinouchi, S. (1995). Cloning, sequencing, and characterization of the gene encoding the smallest subunit of the three-component membrane-bound alcohol dehydrogenase from *Acetobacter pasteurianus*. *The Journal of Bacteriology, 177*, 5048–5055.

Kong, H., Gao, C., & Yan, D. (2004). Functionalization of multiwalled carbon nanotubes by atom transfer radical polymerization and defunctionalization of the products. *Macromolecules, 37*, 4022–4030.

Lu, G., Maragakis, P., & Kaxiras, E. (2005). Carbon nanotube interaction with DNA. *Nanoletters, 5*, 897–900.

Lu, Q., Moore, J. M., Huang, G., Mount, A. S., Rao, A. M., Larcom, L. L., et al. (2004). RNA polymer translocation with single-walled carbon nanotubes. *Nanoletters, 4*, 2473–2477.

Magrez, A., Kasas, S., Salicio, V., Pasquier, N., Seo, J. W., Celio, M., et al. (2006). Cellular toxicity of carbon-based nanomaterials. *Nanoletters, 6*, 1121–1125.

Male, K. B., Hrapovic, S., Santini, J. M., & Luong, J. H. T. (2007). Biosensor for arsenite using arsenite oxidase and multiwalled carbon nanotube modified electrodes. *Analytical Chemistry, 79*, 7831–7837.

Mihranyan, A., Llagostera, A. P., Karmhag, R., Stromme, M., & Ek, R. (2004). Moisture sorption by cellulose powders of varying crystallinity. *International Journal of Pharmaceutics, 269*, 433–442.

Moon, S.-H., Park, J.-M., Chun, H.-Y., & Kim, S.-J. (2006). Comparisons of physical properties of bacterial cellulises produced in different culture condition using saccharified food wastes. *Biotechnology and Bioprocess Engineering, 11*, 26–31.

Prato, M., Kostarelos, K., & Bianco, A. (2007). Functionalized carbon nanotubes in drug design and discovery. *Accounts of Chemical Research, 41*, 60–68.

Qiao, Y., Li, C. M., Bao, S.-J., & Bao, Q.-L. (2007). Carbon nanotube/polyaniline composite as anode material for microbial fuel cells. *Journal of Power Sources, 170*, 79–84.

Sayes, C. M., Liang, F., Hudson, J. L., Mendez, J., Guo, W., Beach, J. M., et al. (2006). Functionalization density dependence of single-walled carbon nanotubes cytotoxicity in vitro. *Toxicology Letters, 161*, 135–142.

Smart, S. K., Cassady, A. I., Lu, G. Q., & Martin, D. J. (2006). The biocompatibility of carbon nanotubes. *Carbon, 44*, 1034–1047.

Terayama, H., Hirota, K., Yoshimura, T., & Esumi, K. (2002). Effect of dilution on aqueous dispersion of drug particles. *Colloid Surface B: Biointerfaces, 27*, 177–180.

Tokoh, C., Takabe, K., Fujita, M., & Saiki, H. (1998). Cellulose synthesized by *Acetobacter xylinum* in the presence of acetyl glucomannan. *Cellulose, 5*, 249–261.

Yan, Z., Chen, S., Wang, H., Wang, B., Wang, C., & Jiang, J. (2008). Cellulose synthesized by *Acetobacter xylinum* in the presence of multi-walled carbon nanotubes. *Carbohydrate Research, 343*, 73–80.

Yoon, S. H., Jin, H.-J., Kook, M.-C., & Pyun, Y. R. (2006). Electrically conductive bacterial cellulose by incorporation of carbon nanotubes. *Biomacromolecules, 7*, 1280–1284.

Zhao, B., Hu, H., Yu, A., Perea, D., & Haddon, R. C. (2005). Synthesis and characterization of water soluble single-walled carbon nanotube graft copolymers. *Journal of the American Chemical Society, 127*, 8197–8203.

Zhou, L. L., Sun, D. P., Hu, L. Y., Li, Y. W., & Yang, J. Z. (2007). Effect of addition of sodium alginate on bacterial cellulose production by *Acetobacter xylinum*. *Journal of Industrial Microbiology and Biotechnology, 34*, 483–489.